arXiv:1605.05497v1 [hep-ph] 18 May 2016

Light sterile neutrino sensitivity of ^{163}Ho experiments

L. Gastaldo[1], C. Giunti[2], and E. M. Zavanin[2,3,4]
[1] *Kirchhoff Institute for Physics, Heidelberg University, INF 227, 69120 Heidelberg, Germany*
[2] *INFN, Sezione di Torino, Via P. Giuria 1, I–10125 Torino, Italy*
[3] *Department of Physics, University of Torino, Via P. Giuria 1, I–10125 Torino, Italy*
[4] *Instituto de Física Gleb Wataghin, Universidade Estadual de Campinas - UNICAMP, Rua Sérgio Buarque de Holanda, 777, 13083-859 Campinas SP Brazil*
(Dated: 18 May 2016)

We explore the sensitivity of ^{163}Ho electron capture experiments to neutrino masses in the standard framework of three-neutrino mixing and in the framework of 3+1 neutrino mixing with a sterile neutrino which mixes with the three standard active neutrinos, as indicated by the anomalies found in short-baseline neutrino oscillations experiments. We calculate the sensitivity to neutrino masses and mixing for different values of the energy resolution of the detectors, of the unresolved pileup fraction and of the total statistics of events, considering the expected values of these parameters in the two planned stages of the ECHo project (ECHo-1k and ECHo-1M). We show that an extension of the ECHo-1M experiment with the possibility to collect 10^{16} events will be competitive with the KATRIN experiment. This statistics will allow to explore part of the 3+1 mixing parameter space indicated by the global analysis of short-baseline neutrino oscillation experiments. In order to cover all the allowed region, a statistics of about 10^{17} events will be needed.

I. INTRODUCTION

The observation of neutrino oscillations is a clear demonstration that neutrinos are massive particles. The data of solar, atmospheric and long-baseline neutrino oscillation experiments are explained in the standard scheme of three-neutrino mixing (3ν) in which the three active neutrinos ν_e, ν_μ, ν_τ are unitary linear combinations of the three massive neutrinos ν_1, ν_2, ν_3, with respective masses m_1, m_2, m_3 (see Refs. [1, 2]). A global analysis of the data of solar, atmospheric and long-baseline neutrino oscillation experiments [3–5] leads to an accurate determination of the three mixing angles and of the two independent solar and atmospheric squared-mass differences, $\Delta m^2_{\text{SOL}} = \Delta m^2_{21} \simeq 7.4 \times 10^{-5}\,\text{eV}^2$ and $\Delta m^2_{\text{ATM}} = |\Delta m^2_{31}| \simeq |\Delta m^2_{32}| \simeq 2.50 \times 10^{-3}\,\text{eV}^2$ [5], with $\Delta m^2_{kj} \equiv m^2_k - m^2_j$.

The 3ν paradigm is presently challenged by anomalies found in short-baseline (SBL) neutrino oscillation experiments: the reactor antineutrino anomaly [6–8], which is a deficit of the rate of $\bar\nu_e$ events measured in reactor neutrino experiments; the Gallium neutrino anomaly [9–13], consisting in a deficit of the rate of ν_e events measured in the Gallium radioactive source experiments GALLEX [14] and SAGE [15]; the LSND anomaly, which is an excess of the rate of $\bar\nu_e$ events in a beam composed mainly of $\bar\nu_\mu$'s produced by μ^+ decay at rest [16, 17]. These anomalies cannot be explained by neutrino oscillations in the 3ν scenario. A possible explanation, still in the framework of neutrino oscillations, requires the existence of a new short-baseline squared-mass difference $\Delta m^2_{\text{SBL}} \gtrsim 1\,\text{eV}^2$, which is much larger than the solar and atmospheric squared-mass differences. The new short-baseline squared-mass difference requires the existence of at least one new massive neutrino ν_4 with mass m_4 such that $\Delta m^2_{\text{SBL}} = |\Delta m^2_{41}|$ (see the review in Ref. [18]). In the flavor basis there must be a sterile neutrino ν_s and the mixing of the left-handed neutrino fields is given by

$$\nu_{\alpha L} = \sum_{k=1}^{4} U_{\alpha k} \nu_{kL} \qquad (\alpha = e, \mu, \tau, s), \tag{1}$$

where U is the unitary 4×4 mixing matrix. In this so-called 3+1 scenario the new massive neutrino must be mainly sterile in order not to spoil the fit of the data of solar, atmospheric and long-baseline experiments (see the reviews in Refs. [18–23]):

$$|U_{\alpha 4}| \ll 1 \quad \text{for} \quad \alpha = e, \mu, \tau. \tag{2}$$

In other words, the 3+1 scheme must be a perturbation of the standard three-neutrino mixing.

Several experiments are planned to check the existence of eV sterile neutrinos (see the reviews in Refs. [18, 24–30]) with high-precision investigations of neutrino oscillations over short baselines by using very accurate detectors for investigating the disappearance of reactor electron antineutrinos (DANSS [31], NEOS [32], Neutrino-4 [33], PROSPECT [34], SoLid [35], STEREO [36]) and electron neutrinos produced by very intense radioactive sources (BEST [37], CeSOX [38]). New accelerator experiments will perform robust investigations of short-baseline $\overset{(-)}{\nu}_\mu \to \overset{(-)}{\nu}_e$ transitions (JSNS2 [39], SBN [40]) and $\overset{(-)}{\nu}_\mu$ disappearance (KPipe [41], SBN [40]). Moreover, there is an increasing interest in the study of the effects of light sterile neutrinos in neutrinoless double-β decay experiments [13, 42–50], in solar neutrino experiments [13, 23, 51–55], in long-baseline neutrino oscillation experiments [56–64], in atmospheric neutrino experiments [65–74] and in cosmology (see Refs. [18, 75–79]).

Although the data of short-baseline experiments can be explained either with $m_1, m_2, m_3 < m_4$ or $m_4 < m_1, m_2, m_3$, the second case is strongly disfavored by cosmological measurements [80] and by the experimental

bounds on neutrinoless double-β decay (assuming that massive neutrinos are Majorana particles; see Ref. [81]), which favor a scenario with $m_1, m_2, m_3 \ll m_4$. In this paper we consider this scenario, which implies that $m_4^2 \simeq \Delta m_{41}^2 = \Delta m_{\rm SBL}^2 \gtrsim 1\,{\rm eV}$. This relation allows us to compare the results of the experiments measuring directly m_4 with the results of short-baseline neutrino oscillation experiments.

The fact that a heavy massive neutrino ν_4 is mixing with the three light massive neutrinos to compose the electron neutrino can give a very clear fingerprint in the spectra of nuclear beta decay and electron capture. This means that experiments designed for the direct investigation of the electron (anti-)neutrino mass have the possibility to scrutinize the parameter space of active-sterile neutrino mixing indicated by short-baseline experiments. The evidence for the existence of such a sterile neutrino would be a kink in the spectrum positioned at $Q - m_4$ [82–84], where Q is the energy available to the decay, which is given by the difference between the masses of the parent and daughter atoms. The amplitude of this kink is related to the mixing $|U_{e4}|$ that ν_4 has with ν_e.

Presently there are two nuclides which are used for the direct investigation of neutrino masses[1]: tritium (^{3}H) undergoing the beta-decay process $^3{\rm H} \to {}^3{\rm He} + e^- + \bar{\nu}_e$ and holmium (^{163}Ho) undergoing the electron-capture process $e^- + {}^{163}{\rm Ho} \to {}^{163}{\rm Dy} + \nu_e$ (see the reviews in Refs. [85–87]). New generation experiments using these nuclides are expected to reach a sensitivity to sub-eV values of the effective electron neutrino mass. Therefore they can investigate the existence of an eV-scale massive neutrino which has a significant mixing with ν_e. The sensitivity that can be reached by the KATRIN experiment [88, 89] to the signature of ν_4 in the ^{3}H beta spectrum was studied in Refs. [89–93]. These works proved that the KATRIN experiment could, within three years of measuring time and at nominal performance, rule out a large part of the parameters space required to explain the anomalies in short-baseline experiments.

In this paper we investigate the sensitivity of ^{163}Ho electron capture experiments to neutrino masses in the standard framework of three-neutrino mixing and in the framework of 3+1 neutrino mixing with an eV-scale sterile neutrino. We consider in particular the first two planned phases of the ECHo project, ECHo-1k and ECHo-1M [94, 95]. Other ^{163}Ho experimental projects are HOLMES [96], which has a program to investigate small neutrino masses competitive with the ECHo program, and NuMECS [97], which at least for the moment is only aiming at a precise measurement of the ^{163}Ho decay spectrum.

[1] Note that the ^{3}H beta-decay process is sensitive to the antineutrino masses, whereas the ^{163}Ho electron-capture process is sensitive to the neutrino masses. Hence, the comparison of the experimental results of the two processes is a test of the CPT symmetry, which implies the equality of neutrino and antineutrino masses.

The plan of the paper is as follows. In Section II we describe the effect of neutrino masses in ^{163}Ho electron capture. In Section III we describe the characteristics of the ECHo experiment which are relevant for our analysis. In Section IV we present our estimation of the sensitivity of the ECHo experiment to the effective neutrino mass in the 3ν framework. In Section V we calculate the sensitivity of the ECHo experiment to m_4 in the case of 3+1 neutrino mixing and we compare it with the region in the space of the mixing parameters allowed by the global analysis of short-baseline neutrino oscillation data. In Section VI we present our conclusions.

II. ^{163}HO ELECTRON CAPTURE PROCESS

The property that makes ^{163}Ho the best isotope for investigating the electron neutrino mass is the very small energy Q available to the decay. Recently, the Q-value has been precisely determined by Penning trap mass spectrometry to be $Q = 2833 \pm 30_{\rm stat} \pm 15_{\rm syst}$ eV [98]. At the present knowledge, this is the lowest Q for all nuclides undergoing electron capture processes.

In an electron capture process one electron from the ^{163}Ho atomic levels is captured, leading to a transformation of a proton into a neutron and the emission of an electron neutrino. The daughter atom, ^{163}Dy is left in an excited state which, at the leading order, is described by a hole in the shell from which the electron has been captured and one electron more in the $4f$ shell with respect to the ones foreseen for the dysprosium atom in the ground state. The excitation energy can then be released through the emission of x-rays or electrons (Auger or Coster-Kronig transition). We indicate the sum of all the energy released in the electron capture process minus the one taken away by the neutrino as $E_{\rm c}$. This is the quantity that is measured by calorimetric techniques in modern experiments studying the ^{163}Ho decay [99]. The concept of these experiments was initially proposed more then thirty year ago by De Rujula and Lusignoli [100, 101].

The decay scheme can then be divided in the following two steps:

$$^{163}{\rm Ho} \to {}^{163}{\rm Dy}^* + \nu_e, \tag{3}$$

$$^{163}{\rm Dy}^* \to {}^{163}{\rm Dy} + E_{\rm c}. \tag{4}$$

Considering only first order transitions and neglecting the nuclear recoil, the expected spectrum for the excitation energy is characterized by a sum of Breit-Wigner resonances modulated by the phase space factor (see

Refs. [85–87]):

$$\frac{dn_{\rm EC}}{dE_{\rm c}} \propto (Q-E_{\rm c})\sum_{k=1}^{N}|U_{ek}|^2\sqrt{(Q-E_{\rm c})^2-m_k^2} \times \Theta(Q-E_{\rm c}-m_k) \times \sum_i P_i \frac{\Gamma_i/2\pi}{(E_{\rm c}-E_i)^2+\Gamma_i^2/4}. \quad (5)$$

Here, P_i is the probability of electron capture from the i-shell, which has been calculated in Ref. [102] using a fully relativistic approach. It is given by $P_i = |\psi_i(R)|^2 B_i$, where $|\psi_i(R)|^2$ is the square of single electron wave functions of the parent atom at the nuclear radius R and B_i is a correction for electron exchange and overlap. The energy E_i is the peak energy of the i-th resonance, which is given in a first approximation by the difference between the binding energy in the daughter atom of the electron that has been captured and the binding energy of the $4f$ electron: $E_i \simeq E_i^b - E_{4f}^b$. The width Γ_i is the intrinsic width of the resonance, which is related to the half-life of the excited i-state. The Heaviside function $\Theta(Q-E_{\rm c}-m_k)$ ensures the reality of the expression. The parameters describing the atomic excited states are taken from Ref. [102] and listed in Tab. I.

The fraction of the calorimetrically measured spectrum which is mostly affected by finite neutrino masses is the endpoint region, where the emitted neutrino has only a few eV of kinetic energy. In the following, we consider a detector with energy resolution of 5 or 2 eV and we assume that the masses m_1, m_2, m_3 of the three massive neutrinos ν_1, ν_2, ν_3, in the framework of the standard three-neutrino mixing scenario, are much smaller than the energy resolution. In this case, Eq. (5) can be approximated by

$$\left(\frac{dn_{\rm EC}}{dE_{\rm c}}\right)_{3\nu} \propto (Q-E_{\rm c})\sqrt{(Q-E_{\rm c})^2-m_\nu^2} \times \Theta(Q-E_{\rm c}-m_\nu) \times \sum_i P_i \frac{\Gamma_i/2\pi}{(E_{\rm c}-E_i)^2+\Gamma_i^2/4}, \quad (6)$$

with the effective electron neutrino mass

$$m_\nu^2 = \sum_{k=1}^{3}|U_{ek}|^2 m_k^2 \quad (7)$$

This approximation is consistent with the most stringent upper limits on m_ν found in the Mainz [103] and Troitsk [104] experiments:

$$m_\nu \leq \begin{cases} 2.3\,{\rm eV} & ({\rm Mainz}), \\ 2.05\,{\rm eV} & ({\rm Troitsk}), \end{cases} \quad (8)$$

at 95% CL.

TABLE I. Experimental excitation energies E_i of the hole states with their widths Γ_i and $P_i/P_{\rm M1}$. Data taken from Ref. [102].

Level i	E_i (eV)	Γ_i (eV)	$P_i/P_{\rm M1}$
M1	2040	13.7	1
M2	1836	7.2	0.051
N1	411	5.3	0.244
N2	333	8.0	0.012
O1	48	4.3	0.032

III. THE ECHO EXPERIMENT

The ECHo experiment is designed to reach a sub-eV sensitivity to the electron neutrino mass through the analysis of the endpoint region of the ^{163}Ho spectrum. The concept at the basis of this experiment is that all the energy released during the ^{163}Ho electron capture, besides that taken away by the neutrino, is measured with high precision. Large arrays of low temperature metallic magnetic calorimeters (MMCs) [105] will be used. The ^{163}Ho atoms will be completely enclosed in the energy absorber, which consists of a gold film with about 10 μm thickness and a $200 \times 200\,\mu{\rm m}^2$ surface area. Such an absorber is thermally coupled to a temperature sensor, which is a thin film of a paramagnetic material, typically gold doped with a few hundreds ppm of erbium, sitting in an external stable magnetic field. The sensor is then weakly coupled to the thermal bath kept at a constant temperature of less then 30 mK. When energy is deposited in the detector, its temperature increases leading to a change of magnetization of the sensor which is read out as a change of flux by low-noise high-bandwidth dc-SQUIDs (Superconducting QUantum Interference Devices). An energy resolution as good as 1.6 eV FWHM at 6 keV has already been achieved with MMCs developed for soft x-ray spectroscopy as well as very precise calibration functions [106]. An intrinsic background is the unresolved pileup which is related to the finite time resolution of the detector and to the fact that, since the ^{163}Ho is enclosed in the detector itself, each ^{163}Ho decay leads to a signal. Therefore, two or more events which occur in a time interval shorter than the risetime of the pulse are misidentified as a single event with an energy given approximately by the sum of the single event energies. The fraction of pileup events is given by the product of the activity in the detector and the risetime of the signal. In order to be able to investigate small neutrino masses, the unresolved pileup fraction $f_{\rm pp}$ should be smaller than 10^{-5}. The first prototypes of MMCs with embedded ^{163}Ho have already shown a risetime of the order of 100 ns [107], which allows for single pixel activities of the order of a few tens of Bq. The goal of the ECHo experiment is to have the sum of all other background contributions in the endpoint region of the spectrum at least one order of magnitude smaller than the unresolved pileup. This corresponds to a background parameter $b < 5 \times 10^{-5}$ counts/eV/det/day.

During the first phase of the ECHo experiment, ECHo-1k, which already started, more then 10^{10} events of ^{163}Ho electron capture will be collected in one year of measuring time by having a ^{163}Ho source of the order of 1000 Bq distributed into about 100 MMCs. The major goals of this phase are to obtain an energy resolution better than 5 eV FWHM for multiplexed detectors and an unresolved pileup fraction smaller than 10^{-5}. Achieving these goals will allow the ECHo Collaboration to reach a limit on the electron neutrino mass below 10 eV, which is more than one order of magnitude better than the current limit on the electron neutrino mass obtained with a ^{163}Ho electron capture experiment, $m_\nu < 225$ eV at 95% C.L. [108].

In the second phase of ECHo, called ECHo-1M, a ^{163}Ho source of the order of 1 MBq will be embedded in a large number of pixels divided into multiplexed arrays. The aim of this phase is to measure a ^{163}Ho spectrum with about 10^{14} events with an energy resolution better that 2 eV FWHM and an unresolved pileup fraction of the order of 10^{-6}. With ECHo-1M the sensitivity to the electron neutrino mass will reach the sub-eV region [109].

The discussed sensitivities are based on the analysis of simulated ^{163}Ho spectra which are generated using only the first order excited states in ^{163}Dy. Higher order excited states, like the one corresponding to the formation of two holes in the ^{163}Dy atom after the electron capture, even if they have a much smaller probability to occur, can play a quite important role in the region near the endpoint of the spectrum. The role of higher order excitations has been recently studied in Refs. [110–113]. There is still not a good agreement among the different authors on the expected structures in the ^{163}Ho spectrum due to these excitations. The available data on the ^{163}Ho spectrum [97, 114, 115] are still not able to clearly resolve the controversy. An important point to mention is that the two-hole excitations in which an electron is "shaken-off" in the continuum may imply a substantial increase of the fraction of events in the endpoint region of the spectrum [112, 113]. Therefore, by presenting limits on the sensitivity based only on the first order excited states, we provide upper values of the sensitivity that could be reached with a well-defined experimental configuration.

IV. 3ν MIXING

In this section we describe our methodology to obtain the sensitivity for the neutrino mass in the ECHo experiment and we present our results for the sensitivity to m_ν in the standard case of three-neutrino mixing. Previous analyses of the sensitivity of ^{163}Ho experiments with various configurations have been presented in Refs. [99, 116–118].

The theoretical spectrum of ^{163}Ho electron capture events as a function of the total released energy E_c is given by

$$\frac{dn}{dE_c}(m_\nu) = N_{ev} S_{tot}(E_c, m_\nu) \otimes R_{\Delta E}(E_c) + B, \qquad (9)$$

with the normalized total spectrum

$$S_{tot}(E_c, m_\nu) = (1 + f_{pp})^{-1} \left[S_{EC}(E_c, m_\nu) + f_{pp} S_{EC}(E_c, m_\nu) \otimes S_{EC}(E_c, m_\nu) \right]. \qquad (10)$$

Here $S_{EC}(E_c, m_\nu)$ is the normalized electron-capture spectrum

$$S_{EC}(E_c, m_\nu) = \left(\frac{dn_{EC}}{dE_c} \right)_{3\nu} \left(\int_0^{Q-m_\nu} \left(\frac{dn_{EC}}{dE_c} \right)_{3\nu} dE_c \right)^{-1}, \qquad (11)$$

with dn_{EC}/dE_c given by Eq. (5). Other quantities in Eqs. (9) and (10) are: the total number of events N_{ev}, which in a real experiment is given by $N_{ev} = N_{det} A t_m$, where N_{det} is the number of detectors, A is the activity of the ^{163}Ho source in each detector and t_m is the measuring time; the background[2] $B = b t_m$; the fraction of pileup events f_{pp}, that, in a first approximation, is given by $f_{pp} = \tau_R A$, where τ_R is the time resolution. The detector energy response $R_{\Delta E}(E_c)$ is assumed to be Gaussian:

$$R_{\Delta E}(E_c) = \frac{1}{\sigma_{\Delta E}\sqrt{2\pi}} \exp\left(-E_c^2 / 2\sigma_{\Delta E}^2\right), \qquad (12)$$

with variance relate to the full width at half maximum by the usual relation $\sigma_{\Delta E} = \Delta E_{FWHM}/2.35$. In Eqs. (9) and (10), the symbol $\otimes$ represents a convolution. The self-convolution of the normalized spectrum in the second term of Eq. (10) accounts for the pileup effect. In order to speed up the computer-intensive evaluation of the sensitivity to m_ν, in this term we used the normalized spectrum $S_{EC}(E_c, 0)$, neglecting the small effects due to m_ν.

Figure 1 illustrates the effect of an effective neutrino mass $m_\nu = 1$ eV on the spectrum S_{EC} and on the total spectrum S_{tot} without and with the convolution with the detector energy response $R_{\Delta E}(E_c)$ for $\Delta E_{FWHM} = 2$ eV. One can see that in the limit of negligible unresolved pileup, represented by the curves labeled S_{EC}, the difference between the spectra with $m_\nu = 0$ and $m_\nu = 1$ eV without and with the convolution with the detector energy response is similar. On the other hand, the difference of the total spectra S_{tot} for $m_\nu = 0$ and $m_\nu = 1$ eV is significantly affected by the energy resolution of the detector. Without considering the finite energy resolution of the detector, the difference between $S_{tot}(m_\nu = 0)$ and $S_{tot}(m_\nu = 1\,\text{eV})$ is relatively large around $Q - m_\nu$, where $S_{EC}(m_\nu = 1\,\text{eV})$ vanishes and only the pileup contributes. Since this difference is strongly reduced by the convolution with the detector energy response, it is clear that the sensitivity to the neutrino mass depends on the energy resolution of the detector. However, the effects

[2] For simplicity, we assume an energy-independent background. If the background has an energy dependence it must be included in the convolution with the energy resolution.

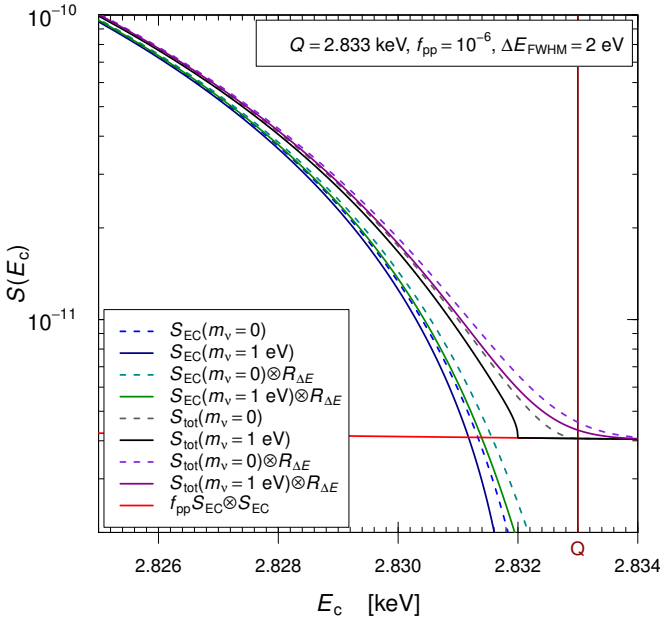

FIG. 1. Energy spectra calculated without and with the convolution with the detector energy response $R_{\Delta E}(E_c)$ for $m_\nu = 0$ and for $m_\nu = 1\,\mathrm{eV}$.

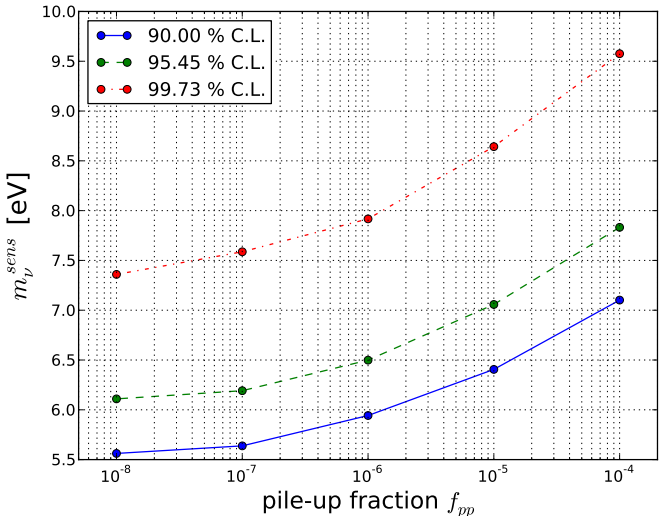

FIG. 2. Estimated sensitivity to m_ν in the ECHo-1k experiment as a function of the pileup fraction f_{pp}. We used $N_{\mathrm{sim}} = 1000$ simulations generated with $N_{\mathrm{ev}} = 10^{10}$, $Q = 2.833$ keV, $\Delta E_{\mathrm{FWHM}} = 5$ eV and $B = 0$.

of a poor energy resolution can be counterbalanced by a large statistics N_{ev} which allows to distinguish the difference between $dn/dE_c(m_\nu \neq 0)$ and $dn/dE_c(m_\nu = 0)$. Indeed, since the difference is proportional to N_{ev}, the Poisson fluctuations of the event numbers in the energy bins are proportional to $\sqrt{N_{\mathrm{ev}}}$ and the sensitivity to m_ν^2 is proportional to $N_{\mathrm{ev}}^{-1/2}$, leading to a sensitivity to m_ν proportional to $N_{\mathrm{ev}}^{-1/4}$ (see also the discussions in Refs. [87, 116]).

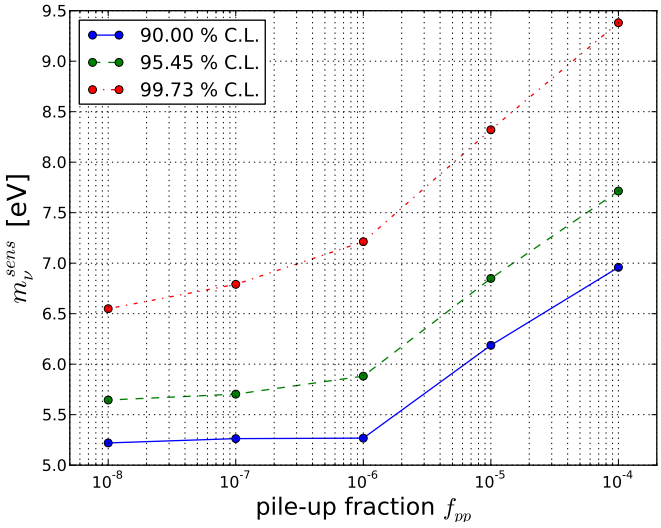

FIG. 3. Estimated sensitivity to m_ν as a function of the pileup fraction f_{pp} in the beginning of the the ECHo-1M experiment when the same statistics of $N_{\mathrm{ev}} = 10^{10}$ expected in the ECHo-1k will be reached. We used $N_{\mathrm{sim}} = 1000$ simulations generated with $Q = 2.833$ keV, $\Delta E_{\mathrm{FWHM}} = 2$ eV and $B = 0$.

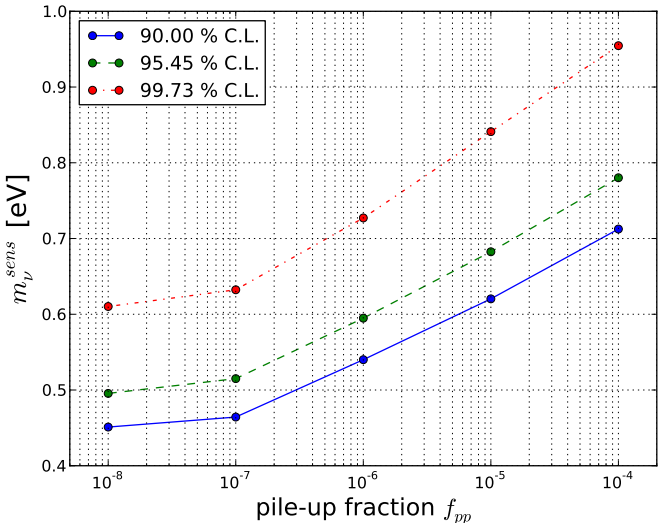

FIG. 4. Estimated sensitivity to m_ν in the ECHo-1M experiment as a function of the pileup fraction f_{pp}. We used $N_{\mathrm{sim}} = 1000$ simulations generated with $N_{\mathrm{ev}} = 10^{14}$, $Q = 2.833$ keV, $\Delta E_{\mathrm{FWHM}} = 2$ eV and $B = 0$.

We computed the sensitivity m_ν^{sens} to m_ν of a given experimental configuration defined by the energy resolution of the detectors, the unresolved pileup fraction and the total statistics. We adopted the Feldman-Cousins definition of sensitivity[3] given in Ref. [119]: "the sensitivity is defined as the average upper limit one would get from an

[3] Note that our definition of sensitivity is different of that used in Refs. [116–118].

ensemble of experiments with the expected background and no true signal." Hence, for a given experimental configuration we generated $N_{\rm sim}$ simulations of the data in the case $m_\nu = 0$, for each simulation we found the corresponding upper limit for m_ν, and we calculated the sensitivity as the median of these upper limits. We did not use the mean of the upper limits, which may be interpreted as the "average" in the Feldman-Cousins definition of sensitivity, because the mean is not defined in the case of limits on more than one parameter, as in the case of 3+1 neutrino mixing considered in Section V. On the other hand, for $N_{\rm par}$ parameters the median is defined as the $N_{\rm par}$ hypersurface which encloses all the values of the parameters which are allowed by more than 50% of the simulations[4].

We considered two experimental configurations corresponding to the expected performances of the ECHo-1k and ECHo-1M experiments [94, 95]. For ECHo-1k we considered $\Delta E_{\rm FWHM} = 5\,{\rm eV}$ and $N_{\rm ev} = 10^{10}$, whereas for ECHo-1M we considered $\Delta E_{\rm FWHM} = 2\,{\rm eV}$ and $N_{\rm ev} = 10^{14}$. We considered different values of the pileup fraction $f_{\rm pp}$ from 10^{-8} to 10^{-4}. We also neglected the background B, which in the ECHo experiment is expected to be at least one order of magnitude smaller than the unresolved pileup, as already mentioned above (see also the discussion in Ref. [118]).

The simulations have been generated with $Q = 2.833\,{\rm keV}$ and the simulated data have been fitted from $E_{\rm c}^{\rm min} = 2.2\,{\rm keV}$ to $E_{\rm c}^{\rm max} = 3.2\,{\rm keV}$ with different bin sizes. We checked that the results are independent of the bin size as long as it is smaller than the energy resolution uncertainty $\sigma_{\Delta E}$.

The theoretical average number of events in the $i^{\rm th}$ energy bin (with $i = 1, \ldots, N_{\rm bins}$) is given by

$$n_i^{\rm th}(m_\nu) = \int_{E_i^{\rm min}}^{E_i^{\rm max}} \frac{dn}{dE_{\rm c}}(m_\nu)\, dE_{\rm c}, \qquad (13)$$

where $E_i^{\rm min}$ and $E_i^{\rm max}$ are, respectively, the lower and upper borders of the bin. In the $j^{\rm th}$ simulation of the data (with $j = 1, \ldots, N_{\rm sim}$), the number of events $(n_i^{\rm sim})_j$ in the $i^{\rm th}$ bin is obtained with a Poisson fluctuation around the theoretical average number of events $n_i^{\rm th}(0)$, corresponding to $m_\nu = 0$. The χ^2 of the $j^{\rm th}$ simulation is given by

$$\chi^2_j(m_\nu) = 2 \sum_{i=1}^{N_{\rm bins}} n_i^{\rm th}(m_\nu) - (n_i^{\rm sim})_j + (n_i^{\rm sim})_j \ln\left(\frac{(n_i^{\rm sim})_j}{n_i^{\rm th}(m_\nu)}\right). \qquad (14)$$

Although specific values of Q, $N_{\rm ev}$, $f_{\rm pp}$ and B have to be used for the generation of the simulated $(n_i^{\rm sim})_j$, we do not make any assumption for the values of these parameters in the expression of $n_i^{\rm th}(m_\nu)$ used in the fit of the simulated data and $\chi^2_j(m_\nu)$ is calculated by marginalizing over them. This method reflects the probable real experimental approach, in which these parameters will be determined by the data[5].

For each simulation j we compute the upper limit $(m_\nu^{\rm UL})_j$ for m_ν at CL confidence level using the relation:

$$\chi^2_j((m_\nu^{\rm UL})_j) = (\chi^2_j)_{\rm min} + \Delta\chi^2(CL), \qquad (15)$$

where $(\chi^2_j)_{\rm min}$ is the minimum of $\chi^2_j(m_\nu)$ and $\Delta\chi^2(CL) = 2.71, 4.0, 9.0$ for $CL = 90\%, 95.45\%, 99.73\%$, respectively. As explained above, the sensitivity $m_\nu^{\rm sens}$ is given by the median of the upper limits $(m_\nu^{\rm UL})_j$ in the ensemble of $N_{\rm sim}$ simulations.

For the first stage of the ECHo experiment, ECHo-1k, the aim is to achieve a total statistics of $N_{\rm ev} \simeq 10^{10}$ with an energy resolution $\Delta E_{\rm FWHM} \simeq 5$ eV. Figure 2 shows our estimation of the sensitivity to m_ν of ECHo-1k as a function of $f_{\rm pp}$. One can see that for the foreseen value $f_{\rm pp} \simeq 10^{-6}$ the sensitivity will be around 6.5 (7.9) eV at 2σ (3σ), which will represent an improvement of more than one order of magnitude with respect to the current limit $m_\nu < 225$ eV at 2σ [108] obtained with a ^{163}Ho electron capture experiment. One can also notice that the sensitivity does not improve much decreasing the value of $f_{\rm pp}$ below about 10^{-6}. This happens for the following two reasons:

1. The relative contribution of the pileup to the number of events is negligible in an energy interval of the order of the energy resolution $\Delta E_{\rm FWHM}$ near the endpoint. Indeed, near the endpoint $S_{\rm EC} \propto \Delta E^2_{\rm FWHM}/Q^3$ and the number of events in the energy interval $\Delta E_{\rm FWHM}$ is proportional to $(\Delta E_{\rm FWHM}/Q)^3$. On the other hand, since typically the pileup is due to two events with energies well below the endpoint, where $Q - E_{\rm c}$ is large, the number of pileup events in the energy interval $\Delta E_{\rm FWHM}$ is proportional to $f_{\rm pp}\Delta E_{\rm FWHM}/2Q$. Hence, the pileup is negligible near the endpoint for $f_{\rm pp} \ll 2(\Delta E_{\rm FWHM}/Q)^2$, i.e. $f_{\rm pp} \ll 5 \times 10^{-6}$ for $\Delta E_{\rm FWHM} \simeq 5$ eV.

2. The average number of pileup events in an energy interval of the order of the energy resolution $\Delta E_{\rm FWHM}$ near the endpoint is smaller than one. Indeed, neglecting the small effects due to the neutrino mass, the average number of pileup events in

[4] Note, however, that in the one-parameter case the distinction is practically irrelevant if the fluctuations of the simulations follow a Gaussian distribution, for which the mean is equal to the median. In our case we use a Poisson distribution, but since the number of events in the bins are large if the pileup is not too small, the distinction between median and mean is negligible in our analysis.

[5] We kept fixed the energy and width of the M1 Breit-Wigner resonance whose tail determines the spectrum in the energy range of the fits. These parameters will be measured independently with high precision in ECHo and other ^{163}Ho experiments.

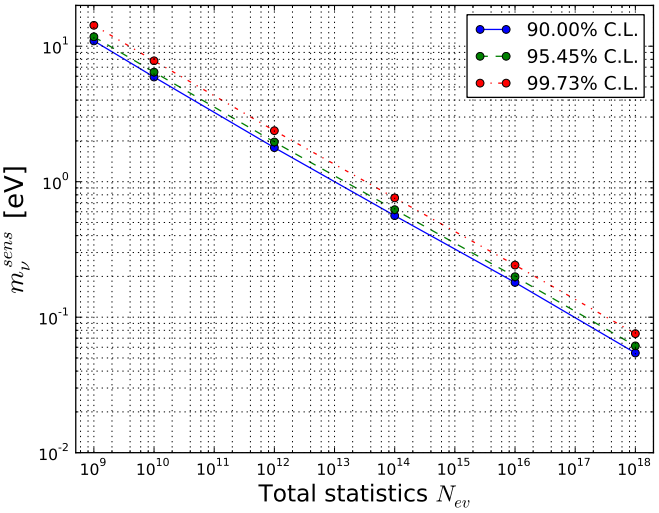

FIG. 5. Estimated sensitivity to m_ν as a function of the statistics $N_{\rm ev}$. We used $N_{\rm sim} = 1000$ simulations generated with $Q = 2.833$ keV, $\Delta E_{\rm FWHM} = 2$ eV, $f_{\rm pp} = 10^{-6}$ and $B = 0$.

the energy interval $\Delta E_{\rm FWHM}$ is smaller than one for

$$f_{\rm pp} \lesssim \left[N_{\rm ev} S_{\rm EC}(E_{\rm c},0) \otimes S_{\rm EC}(E_{\rm c},0) \Delta E_{\rm FWHM}\right]^{-1}. \quad (16)$$

Since near the endpoint we have $S_{\rm EC}(E_{\rm c},0) \otimes S_{\rm EC}(E_{\rm c},0) = 4.07 \times 10^{-6}$, for $N_{\rm ev} = 10^{10}$ and $\Delta E_{\rm FWHM} \simeq 5$ eV we obtain the condition $f_{\rm pp} \lesssim 5 \times 10^{-7}$.

In the second stage of the ECHo experiment, ECHo-1M, it is expected to have an energy resolution better than $\Delta E_{\rm FWHM} = 2$ eV. Figure 3 shows our estimation of the sensitivity to m_ν of ECHo-1M as a function of $f_{\rm pp}$ when the same statistics of $N_{\rm ev} = 10^{10}$ expected in the ECHo-1k will be reached. Comparing Figs. 2 and 3, one can see that the improvement of the energy resolution generates a small improvement of the sensitivity. One can also notice a flatter behavior of the sensitivity for $f_{\rm pp} \lesssim 10^{-6}$ in Fig. 3 than in Fig. 2. This is due to the fact that albeit the condition 1 above is satisfied for $f_{\rm pp} \ll 1 \times 10^{-6}$, the condition 2 is already satisfied for $f_{\rm pp} \lesssim 1 \times 10^{-6}$.

Figure 4 shows our estimation of the final sensitivity to m_ν of ECHo-1M as a function of $f_{\rm pp}$ when the statistics of $N_{\rm ev} = 10^{14}$ will be reached. One can see that it is possible to reach a sensitivity of about 0.6 (0.7) eV at 2σ (3σ) for the foreseen value $f_{\rm pp} \simeq 10^{-6}$. Hence, ECHo-1M will enter into the sub-eV region of m_ν, not far from the expected 0.2 eV sensitivity of KATRIN [88, 89]. The behavior of the sensitivity for $f_{\rm pp} \lesssim 10^{-6}$ is less flat than those in Fig. 2 and 3 because only the condition 1 above is satisfied for $f_{\rm pp} \ll 1 \times 10^{-6}$, whereas the condition 2 is satisfied only for $f_{\rm pp} \lesssim 1 \times 10^{-10}$.

Figure 5 shows our results for the sensitivity to m_ν as a function of the total statistics $N_{\rm ev}$ for $\Delta E_{\rm FWHM} = 2$ eV, $f_{\rm pp} = 10^{-6}$ and $B = 0$. One can see that $m_\nu^{\rm sens}$ follows the expected proportionality to $N_{\rm ev}^{-1/4}$ explained above, in agreement with the calculations presented in Refs. [87, 118].

In a future experiment larger than ECHo-1M it may be possible to have a total statistics of $N_{\rm ev} \simeq 10^{16}$. Figure 5 shows that in this case it will be possible to reach a sensitivity to m_ν of about 0.2 eV, similar to that expected for the KATRIN experiment [88, 89].

V. 3+1 NEUTRINO MIXING

In this section we present our analysis of the sensitivity of future ^{163}Ho experiments to the effects of the heavy neutrino ν_4 in the 3+1 neutrino mixing scheme considering $m_4 \gg m_k$ for $k = 1, 2, 3$ as explained in the introductory Section I. In this case, Eq. (5) can be approximated by

$$\left(\frac{dn_{\rm EC}}{dE_{\rm c}}\right)_{3+1} \propto (Q - E_{\rm c}) \sum_i P_i \frac{\Gamma_i/2\pi}{(E_{\rm c} - E_i)^2 + \Gamma_i^2/4} \times \Big[(1 - |U_{e4}|^2)\sqrt{(Q - E_{\rm c})^2 - m_\nu^2}\,\Theta(Q - E_{\rm c} - m_\nu) + |U_{e4}|^2 \sqrt{(Q - E_{\rm c})^2 - m_4^2}\,\Theta(Q - E_{\rm c} - m_4)\Big], \quad (17)$$

with m_ν given by Eq. (7). Therefore, the complete spectrum can be described as a sum of two spectra, one ending at $Q - m_\nu$ with a fraction of events given by $(1 - |U_{e4}^2|)$ and the other ending at $Q - m_4$ with a fraction of events given by $|U_{e4}^2|$.

The spectrum in Eq. (17) depends on the three neutrino parameters m_ν, m_4 and $|U_{e4}|^2$ and allows to calculate the sensitivity of a ^{163}Ho in the corresponding three-dimensional parameter space. Here, we simplify the problem by assuming that m_ν is much smaller than the sensitivity of the experiment. Hence, we consider the simplified spectrum

$$\left(\frac{dn_{\rm EC}}{dE_{\rm c}}\right)_{3+1} \propto (Q - E_{\rm c}) \sum_i P_i \frac{\Gamma_i/2\pi}{(E_{\rm c} - E_i)^2 + \Gamma_i^2/4} \times \Big[(1 - |U_{e4}|^2)(Q - E_{\rm c})\,\Theta(Q - E_{\rm c}) + |U_{e4}|^2 \sqrt{(Q - E_{\rm c})^2 - m_4^2}\,\Theta(Q - E_{\rm c} - m_4)\Big], \quad (18)$$

which depends only on m_4 and $|U_{e4}|^2$.

We considered the space of the two parameters $\Delta m_{41}^2 \simeq m_4^2$ and $\sin^2 2\vartheta_{ee} = 4|U_{e4}|^2(1 - |U_{e4}|^2)$ in order to compare the sensitivity of ^{163}Ho experiments with the results of global analyses of short-baseline neutrino oscillation data [18, 22, 55, 120–129]. We calculated the sensitivity of ^{163}Ho experiments in the $\sin^2 2\vartheta_{ee}$–Δm_{41}^2 plane with a method similar to that described in Section IV, using the spectrum in Eq. (18). In the 3+1 case, for each simulation j we compute the allowed region at

CL confidence level in the $\sin^2 2\vartheta_{ee}$–Δm^2_{41} plane using the relation:

$$\chi^2_j(\sin^2 2\vartheta_{ee}, \Delta m^2_{41}) \leq (\chi^2_j)_{\rm min} + \Delta\chi^2(CL), \qquad (19)$$

where $(\chi^2_j)_{\rm min}$ is the minimum of $\chi^2_j(\sin^2 2\vartheta_{ee}, \Delta m^2_{41})$ and $\Delta\chi^2(CL) = 4.61, 6.18, 11.83$ for $CL = 90\%, 95.45\%, 99.73\%$, respectively. We calculate the region of sensitivity in the $\sin^2 2\vartheta_{ee}$–Δm^2_{41} plane as the set of points which are not allowed by the inequality (19) in at least 50% of the simulations (see the discussion on the definition of sensitivity in Section IV).

The results are presented in Fig. 6, where we plotted the sensitivity curves for $N_{\rm ev} = 10^{14}$, 10^{16}, 10^{17} and 10^{18}, considering $Q = 2.833$ keV, $\Delta E_{\rm FWHM} = 2$ eV and $f_{\rm pp} = 10^{-6}$. From Fig. 6 one can see that the sensitivity to Δm^2_{41} worsens decreasing $\sin^2 2\vartheta_{ee}$. Indeed, for small values of $\sin^2 2\vartheta_{ee}$ we have $|U_{e4}|^2 \simeq \sin^2 2\vartheta_{ee}/4$ and the contribution of $m^2_4 \simeq \Delta m^2_{41}$ to the spectrum (18) is suppressed. On the other hand, the sensitivity to $m^2_4 \simeq \Delta m^2_{41}$ for $\sin^2 2\vartheta_{ee} = 1$ is only slightly worse of that for m^2_ν in the three-neutrino mixing case discussed in Section IV, because $\sin^2 2\vartheta_{ee} = 1$ corresponds to $|U_{e4}|^2 = 1/2$.

In Fig. 6 we also depicted the region allowed at 95.45% C.L. by a global fit of short-baseline neutrino oscillation data [18, 126] and the 95.45% C.L. allowed regions obtained by restricting the analysis to the data of ν_e and $\bar\nu_e$ disappearance experiments [13, 130], taking into account the Mainz [131] and Troitsk [132, 133] bounds. These last regions are interesting because it is possible that the disappearance of ν_e and $\bar\nu_e$ indicated by the reactor and Gallium anomalies will be confirmed by the future experiments whereas the LSND anomaly will not.

From Fig. 6 one can see that the ν_e and $\bar\nu_e$ disappearance region is wider than the globally allowed region and extends to values of Δm^2_{41} as large as about 80 eV^2. Hence, it can be partially explored by the ECHo-1M experiment, which is expected to have a statistics of $N_{\rm ev} \simeq 10^{14}$.

Figure 6 shows that in order to explore the region which is allowed by the global fit of short-baseline neutrino oscillation data it will be necessary to make a ^{163}Ho experiment with a statistics $N_{\rm ev} \gtrsim 10^{16}$. One can also see that an ^{163}Ho experiment with this statistics will be competitive with the KATRIN experiment [89], a result that is consistent with that for the sensitivity on m_ν in the standard framework of three-neutrino mixing discussed at the end of Section IV.

Figure 6 also shows that the exploration of the small-Δm^2_{41} regions allowed by the ν_e and $\bar\nu_e$ disappearance data will require a statistics as high as $N_{\rm ev} \approx 10^{18}$.

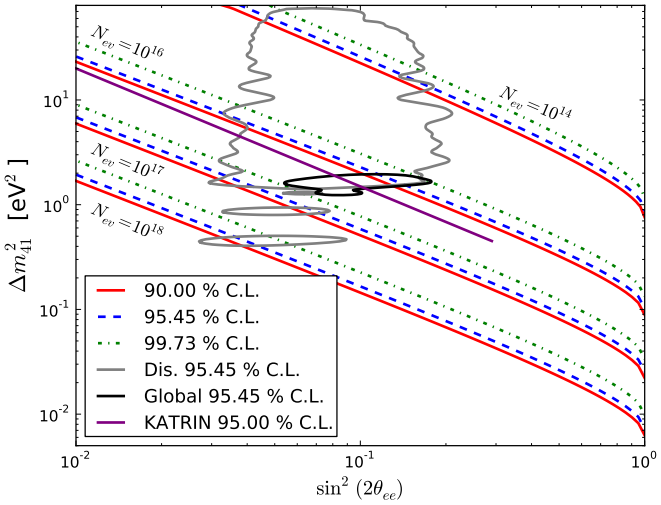

FIG. 6. Estimated sensitivity curves at 90% C.L. (red), 95.45% C.L. (dashed blue) and 99.73% C.L. (dash-dotted green) in the $\sin^2 2\vartheta_{ee}$–Δm^2_{41} plane in the case of 3+1 neutrino mixing for $N_{\rm ev} = 10^{14}$, 10^{16}, 10^{17} and 10^{18}. We used $N_{\rm sim} = 100$ simulations generated with $Q = 2.833$ keV, $\Delta E_{\rm FWHM} = 2$ eV, $f_{\rm pp} = 10^{-6}$ and $B = 0$. The black curve encloses the region allowed at 95.45% C.L. by a global fit of short-baseline neutrino oscillation data [18, 126]. The gray curves enclose the 95.45% C.L. allowed regions obtained by restricting the analysis to the data of ν_e and $\bar\nu_e$ disappearance experiments [13, 130], taking into account the Mainz [131] and Troitsk [132, 133] bounds. Also shown is the expected 95% C.L. sensitivity of the KATRIN experiment [89].

VI. CONCLUSIONS

In this paper we presented the results of an analysis of the sensitivity of ^{163}Ho experiments to neutrino masses considering first the effective neutrino mass m_ν in the standard framework of three-neutrino mixing (see Eq. (7)) and then an additional mass m_4 at the eV scale in the framework of 3+1 neutrino mixing with a sterile neutrino. We considered the experimental setups corresponding to the two planned stages of the ECHo project, ECHo-1k and ECHo-1M [94, 95].

We found that the ECHo-1k experiment can reach a sensitivity to m_ν of about 6.5 eV at 2σ with a total statistics of $N_{\rm ev} \simeq 10^{10}$, an energy resolution $\Delta E_{\rm FWHM} \simeq 5$ eV and a pileup fraction $f_{\rm pp} \simeq 10^{-6}$. Although this sensitivity is still not competitive with that of tritium-decay experiments, it will represent an improvement of more than one order of magnitude with respect to the current limit $m_\nu < 225$ eV at 2σ [108] obtained with a ^{163}Ho electron capture experiment. We also found that the ECHo-1k experiment will not allow to put more stringent limits on the mass and mixing of ν_4 than those already obtained in the Mainz [131] and Troitsk [132, 133] experiments.

According to our estimation, the second stage of the ECHo project, ECHo-1M, can reach a sensitivity to m_ν of about 0.7 eV at 2σ with $N_{\rm ev} \simeq 10^{14}$, $\Delta E_{\rm FWHM} \simeq 2$ eV and $f_{\rm pp} \simeq 10^{-6}$. This result will narrow the gap between the sensitivities of tritium-decay experiments and ^{163}Ho electron capture experiments. Indeed, 0.7 eV is smaller than the current upper limit of about 2 eV at 2σ obtained in the Mainz [103] and Troitsk [104] experiments and it

is not too far from the expected sensitivity of about 0.2 eV of the KATRIN experiment [88, 89].

We found that the ECHo-1M experiment will be sensitive to the large-$\sin^2 2\vartheta_{ee}$ and large-Δm^2_{41} part of the region in the $\sin^2 2\vartheta_{ee}$–Δm^2_{41} plane which is allowed by the data of short-baseline ν_e and $\bar{\nu}_e$ disappearance experiments [13, 130], taking into account the Mainz [131] and Troitsk [132, 133] bounds. However, it cannot explore the region allowed by the global fit of short-baseline neutrino oscillation data [18, 126].

According to our calculations, a ^{163}Ho electron capture experiment with $\Delta E_{\rm FWHM} \simeq 2$ eV and $f_{\rm pp} \simeq 10^{-6}$ will be competitive with the KATRIN tritium-decay experiment [88, 89] by reaching a statistics of $N_{\rm ev} \approx 10^{16}$. Such an experiment will cover a large part of the region in the $\sin^2 2\vartheta_{ee}$–Δm^2_{41} plane which is allowed by the data of short-baseline ν_e and $\bar{\nu}_e$ disappearance experiments and the large-$\sin^2 2\vartheta_{ee}$ and large-Δm^2_{41} part of the region allowed by the global fit of short-baseline neutrino oscillation data.

In order to explore all the region allowed by the global fit of short-baseline neutrino oscillation it will be necessary to have a statistics of $N_{\rm ev} \approx 10^{17}$ and to cover all the region allowed by the data of short-baseline ν_e and $\bar{\nu}_e$ disappearance experiments a statistics of $N_{\rm ev} \approx 10^{18}$ will be needed. These large event numbers seem unreachable now, but we think that we should be optimistic, taking into account that the development of ^{163}Ho electron capture experiment is only at the beginning.

ACKNOWLEDGMENTS

We would like to thank A. De Rujula, A. Faessler, M. Lusignoli, A. Nucciotti, T. Schwetz for fruitful discussions. L.G. acknowledges the support by the DFG Research Unit FOR 2202 "Neutrino Mass Determination by Electron Capture in 163Ho, ECHo" (funding under GA 2219/2-1). The work of C.G. was partially supported by the research grant *Theoretical Astroparticle Physics* number 2012CPPYP7 under the program PRIN 2012 funded by the Ministero dell'Istruzione, Università e della Ricerca (MIUR). E.Z. thanks the support of funding grants 2013/02518-7 and 2014/23980-3, São Paulo Research Foundation (FAPESP).

[1] G. Bellini, L. Ludhova, G. Ranucci, and F. Villante, Adv.High Energy Phys. **2014**, 191960 (2014), arXiv:1310.7858.
[2] Y. Wang and Z. zhong Xing, arXiv:1504.06155.
[3] D. V. Forero, M. Tortola, and J. W. F. Valle, Phys.Rev. **D90**, 093006 (2014), arXiv:1405.7540.
[4] J. Bergstrom, M. C. Gonzalez-Garcia, M. Maltoni, and T. Schwetz, JHEP **09**, 200 (2015), arXiv:1507.04366.
[5] F. Capozzi, E. Lisi, A. Marrone, D. Montanino, and A. Palazzo, arXiv:1601.07777.
[6] T. A. Mueller *et al.*, Phys. Rev. **C83**, 054615 (2011), arXiv:1101.2663.
[7] G. Mention *et al.*, Phys. Rev. **D83**, 073006 (2011), arXiv:1101.2755.
[8] P. Huber, Phys. Rev. **C84**, 024617 (2011), arXiv:1106.0687.
[9] SAGE, J. N. Abdurashitov *et al.*, Phys. Rev. **C73**, 045805 (2006), nucl-ex/0512041.
[10] M. Laveder, Nucl. Phys. Proc. Suppl. **168**, 344 (2007).
[11] C. Giunti and M. Laveder, Mod. Phys. Lett. **A22**, 2499 (2007), hep-ph/0610352.
[12] C. Giunti and M. Laveder, Phys. Rev. **C83**, 065504 (2011), arXiv:1006.3244.
[13] C. Giunti, M. Laveder, Y. Li, Q. Liu, and H. Long, Phys. Rev. **D86**, 113014 (2012), arXiv:1210.5715.
[14] F. Kaether, W. Hampel, G. Heusser, J. Kiko, and T. Kirsten, Phys. Lett. **B685**, 47 (2010), arXiv:1001.2731.
[15] SAGE, J. N. Abdurashitov *et al.*, Phys. Rev. **C80**, 015807 (2009), arXiv:0901.2200.
[16] LSND, C. Athanassopoulos *et al.*, Phys. Rev. Lett. **75**, 2650 (1995), nucl-ex/9504002.
[17] LSND, A. Aguilar *et al.*, Phys. Rev. **D64**, 112007 (2001), hep-ex/0104049.
[18] S. Gariazzo, C. Giunti, M. Laveder, Y. Li, and E. Zavanin, J. Phys. **G43**, 033001 (2016), arXiv:1507.08204.
[19] S. M. Bilenky, C. Giunti, and W. Grimus, Prog. Part. Nucl. Phys. **43**, 1 (1999), hep-ph/9812360.
[20] M. C. Gonzalez-Garcia and M. Maltoni, Phys. Rept. **460**, 1 (2008), arXiv:0704.1800.
[21] K. N. Abazajian *et al.*, arXiv:1204.5379.
[22] J. Conrad, C. Ignarra, G. Karagiorgi, M. Shaevitz, and J. Spitz, Adv.High Energy Phys. **2013**, 163897 (2013), arXiv:1207.4765.
[23] A. Palazzo, Mod.Phys.Lett. **A28**, 1330004 (2013), arXiv:1302.1102.
[24] T. Lasserre, Nucl. Part. Phys. Proc. **265-266**, 281 (2015).
[25] D. Lhuillier, AIP Conf. Proc. **1666**, 180003 (2015).
[26] B. Caccianiga, AIP Conf. Proc. **1666**, 180002 (2015).
[27] J. Spitz, AIP Conf. Proc. **1666**, 180004 (2015).
[28] C. Giunti, arXiv:1512.04758.
[29] L. Stanco, arXiv:1604.06769.
[30] A. Fava, Reviews in Physics **1**, 52 (2016).
[31] DANSS, M. Danilov, arXiv:1412.0817.
[32] B. R. Kim *et al.*, arXiv:1511.05551.
[33] A. P. Serebrov *et al.*, arXiv:1310.5521.
[34] PROSPECT, J. Ashenfelter *et al.*, arXiv:1512.02202.
[35] SoLid, N. Ryder, PoS **EPS-HEP2015**, 071 (2015), arXiv:1510.07835.
[36] V. Helaine, arXiv:1604.08877.
[37] V. Barinov, V. Gavrin, D. Gorbunov, and T. Ibragimova, Phys.Rev. **D93**, 073002 (2016), arXiv:1602.03826.
[38] Borexino, G. Bellini *et al.*, JHEP **1308**, 038 (2013), arXiv:1304.7721.
[39] M.Harada *et al.*, arXiv:1601.01046.
[40] MicroBooNE, LAr1-ND, ICARUS-WA104, R. Acciarri

et al., arXiv:1503.01520.
[41] S. N. Axani *et al.*, arXiv:1510.06994.
[42] J. Barry, W. Rodejohann, and H. Zhang, JHEP **07**, 091 (2011), arXiv:1105.3911.
[43] Y. Li and S. Liu, Phys. Lett. **B706**, 406 (2012), arXiv:1110.5795.
[44] W. Rodejohann, J. Phys. **G39**, 124008 (2012), arXiv:1206.2560.
[45] I. Girardi, A. Meroni, and S. T. Petcov, JHEP **1311**, 146 (2013), arXiv:1308.5802.
[46] S. Pascoli, M. Mitra, and S. Wong, Phys.Rev. **D90**, 093005 (2014), arXiv:1310.6218.
[47] A. Meroni and E. Peinado, Phys.Rev. **D90**, 053002 (2014), arXiv:1406.3990.
[48] A. Abada, V. D. Romeri, and A. Teixeira, JHEP **1409**, 074 (2014), arXiv:1406.6978.
[49] C. Giunti and E. M. Zavanin, JHEP **07**, 171 (2015), arXiv:1505.00978.
[50] H. Pas and W. Rodejohann, New J. Phys. **17**, 115010 (2015), arXiv:1507.00170.
[51] A. Palazzo, Phys. Rev. **D83**, 113013 (2011), arXiv:1105.1705.
[52] A. Palazzo, Phys. Rev. **D85**, 077301 (2012), arXiv:1201.4280.
[53] H. Long, Y. Li, and C. Giunti, Phys. Rev. D 87, **113004**, 113004 (2013), arXiv:1304.2207.
[54] H. Long, Y. Li, and C. Giunti, JHEP **1308**, 056 (2013), arXiv:1306.4051.
[55] J. Kopp, P. A. N. Machado, M. Maltoni, and T. Schwetz, JHEP **1305**, 050 (2013), arXiv:1303.3011.
[56] A. de Gouvea, K. J. Kelly, and A. Kobach, Phys.Rev. **D91**, 053005 (2015), arXiv:1412.1479.
[57] N. Klop and A. Palazzo, Phys.Rev. **D91**, 073017 (2015), arXiv:1412.7524.
[58] J. M. Berryman, A. de Gouvea, K. J. Kelly, and A. Kobach, Phys. Rev. **D92**, 073012 (2015), arXiv:1507.03986.
[59] R. Gandhi, B. Kayser, M. Masud, and S. Prakash, JHEP **11**, 039 (2015), arXiv:1508.06275.
[60] A. Palazzo, Phys.Lett. **B757**, 142 (2016), arXiv:1509.03148.
[61] S. K. Agarwalla, S. S. Chatterjee, A. Dasgupta, and A. Palazzo, JHEP **02**, 111 (2016), arXiv:1601.05995.
[62] S. K. Agarwalla, S. S. Chatterjee, and A. Palazzo, arXiv:1603.03759.
[63] S. Choubey and D. Pramanik, arXiv:1604.04731.
[64] S. K. Agarwalla, S. S. Chatterjee, and A. Palazzo, arXiv:1605.04299.
[65] S. Razzaque and A. Y. Smirnov, JHEP **07**, 084 (2011), arXiv:1104.1390.
[66] S. Razzaque and A. Y. Smirnov, Phys. Rev. **D85**, 093010 (2012), arXiv:1203.5406.
[67] R. Gandhi and P. Ghoshal, Phys. Rev. **D86**, 037301 (2012), arXiv:1108.4360.
[68] A. Esmaili, F. Halzen, and O. L. G. Peres, JCAP **1211**, 041 (2012), arXiv:1206.6903.
[69] A. Esmaili, F. Halzen, and O. L. G. Peres, JCAP **1307**, 048 (2013), arXiv:1303.3294.
[70] A. Esmaili and A. Y. Smirnov, JHEP **1312**, 014 (2013), arXiv:1307.6824.
[71] S. Rajpoot, S. Sahu, and H. C. Wang, Eur.Phys.J. **C74**, 2936 (2014), arXiv:1310.7075.
[72] M. Lindner, W. Rodejohann, and X.-J. Xu, JHEP **01**, 124 (2016), arXiv:1510.00666.
[73] J. Liao and D. Marfatia, arXiv:1602.08766.
[74] IceCube, M. G. Aartsen *et al.*, arXiv:1605.01990.
[75] J. Lesgourgues, G. Mangano, G. Miele, and S. Pastor, *Neutrino Cosmology* (Cambridge University Press, 2013).
[76] S. Riemer-Sorensen, D. Parkinson, and T. M. Davis, Publ.Astron.Soc.Austral. **30**, e029 (2013), arXiv:1301.7102.
[77] M. Archidiacono, E. Giusarma, S. Hannestad, and O. Mena, Adv.High Energy Phys. **2013**, 191047 (2013), arXiv:1307.0637.
[78] J. Lesgourgues and S. Pastor, New J.Phys. **16**, 065002 (2014), arXiv:1404.1740.
[79] S. Hannestad, arXiv:1605.03829.
[80] Planck, P. A. R. Ade *et al.*, arXiv:1502.01589.
[81] S. Bilenky and C. Giunti, Int.J.Mod.Phys. **A30**, 0001 (2015), arXiv:1411.4791.
[82] M. Nakagawa, H. Okonogi, S. Sakata, and A. Toyoda, Prog. Theor. Phys. **30**, 727 (1963).
[83] R. E. Shrock, Phys. Lett. **B96**, 159 (1980).
[84] R. E. Shrock, Phys. Rev. **D24**, 1232 (1981).
[85] G. Drexlin, V. Hannen, S. Mertens, and C. Weinheimer, Adv. High Energy Phys. **2013**, 293986 (2013), arXiv:1307.0101.
[86] O. Dragoun and D. Venos, arXiv:1504.07496.
[87] A. Nucciotti, arXiv:1511.00968.
[88] KATRIN, A. Osipowicz *et al.*, hep-ex/0109033.
[89] S. Mertens, (2015), Talk presented at TAUP 2015, 7-11 September 2015, Torino, Italy.
[90] A. S. Riis and S. Hannestad, JCAP **1102**, 011 (2011), arXiv:1008.1495.
[91] J. A. Formaggio and J. Barrett, Phys. Lett. **B706**, 68 (2011), arXiv:1105.1326.
[92] A. S. Riis, S. Hannestad, and C. Weinheimer, Phys. Rev. **C84**, 045503 (2011), arXiv:1105.6005.
[93] A. Esmaili and O. L. G. Peres, Phys. Rev. **D85**, 117301 (2012), arXiv:1203.2632.
[94] L. Gastaldo *et al.*, J.Low Temp.Phys. **176**, 876 (2014), arXiv:1309.5214.
[95] C. Hassel *et al.*, J.Low Temp.Phys. (2016).
[96] B. Alpert *et al.*, Eur.Phys.J. **C75**, 112 (2015), arXiv:1412.5060.
[97] M. P. Croce *et al.*, arXiv:1510.03874.
[98] S. Eliseev *et al.*, Phys.Rev.Lett. **115**, 062501 (2015), arXiv:1604.04210.
[99] L. Gastaldo, AIP Conf. Proc. **1666**, 050001 (2015), arXiv:1409.0894.
[100] A. De Rujula, Nucl. Phys. **B188**, 414 (1981).
[101] A. De Rujula and M. Lusignoli, Phys. Lett. **B118**, 429 (1982).
[102] A. Faessler, L. Gastaldo, and M. Simkovic, J.Phys. **G42**, 015108 (2015), arXiv:1407.6504.
[103] C. Kraus *et al.*, Eur. Phys. J. **C40**, 447 (2005), hep-ex/0412056.
[104] Troitsk, V. Aseev *et al.*, Phys. Rev. **D84**, 112003 (2011), arXiv:1108.5034.
[105] A. Fleischmann, C. Enss, and G. Seidel, *Cryogenic Particle Detection* (Springer Berlin Heidelberg, Berlin, Heidelberg, 2005), chap. Metallic Magnetic Calorimeters, pp. 151–216.
[106] C. Pies *et al.*, Journal of Low Temperature Physics (269-279).
[107] L. Gastaldo *et al.*, Nucl. Instrum. Meth. **A711**, 150 (2013), arXiv:1206.5647.

[108] P. T. Springer, C. L. Bennett, and P. A. Baisden, Phys. Rev. **A35**, 679 (1987).

[109] K. Blaum *et al.*, (2016), To be submitted to EPJ ST.

[110] R. G. H. Robertson, Phys.Rev. **C91**, 035504 (2015), arXiv:1411.2906.

[111] A. Faessler and F. Simkovic, Phys.Rev. **C91**, 045505 (2015), arXiv:1501.04338.

[112] A. D. Rujula and M. Lusignoli, arXiv:1510.05462.

[113] A. D. Rujula and M. Lusignoli, JHEP **1605**, 015 (2016), arXiv:1601.04990.

[114] P. C.-O. Ranitzsch *et al.*, Journal of Low Temperature Physics (1004-1014).

[115] P. C.-O. Ranitzsch *et al.*, arXiv:1409.0071.

[116] A. Nucciotti, E. Ferri, and O. Cremonesi, Astropart. Phys. **34**, 80 (2010), arXiv:0912.4638.

[117] F. Gatti, M. Galeazzi, M. Lusignoli, A. Nucciotti, and S. Ragazzi, arXiv:1202.4763.

[118] A. Nucciotti, Eur.Phys.J. **C74**, 3161 (2014), arXiv:1405.5060.

[119] G. J. Feldman and R. D. Cousins, Phys. Rev. **D57**, 3873 (1998), physics/9711021.

[120] J. Kopp, M. Maltoni, and T. Schwetz, Phys. Rev. Lett. **107**, 091801 (2011), arXiv:1103.4570.

[121] C. Giunti and M. Laveder, Phys.Rev. **D84**, 073008 (2011), arXiv:1107.1452.

[122] C. Giunti and M. Laveder, Phys.Rev. **D84**, 093006 (2011), arXiv:1109.4033.

[123] C. Giunti and M. Laveder, Phys. Lett. **B706**, 200 (2011), arXiv:1111.1069.

[124] M. Archidiacono, N. Fornengo, C. Giunti, and A. Melchiorri, Phys. Rev. **D86**, 065028 (2012), arXiv:1207.6515.

[125] M. Archidiacono, N. Fornengo, C. Giunti, S. Hannestad, and A. Melchiorri, Phys.Rev. **D87**, 125034 (2013), arXiv:1302.6720.

[126] C. Giunti, M. Laveder, Y. Li, and H. Long, Phys.Rev. **D88**, 073008 (2013), arXiv:1308.5288.

[127] C. Giunti and E. M. Zavanin, Mod. Phys. Lett. **A31**, 1650003 (2016), arXiv:1508.03172.

[128] G. H. Collin, C. A. Arguelles, J. M. Conrad, and M. H. Shaevitz, arXiv:1602.00671.

[129] M. Ericson, M. V. Garzelli, C. Giunti, and M. Martini, Phys.Rev. **D93**, 073008 (2016), arXiv:1602.01390.

[130] C. Giunti, M. Laveder, Y. Li, and H. Long, Phys. Rev. **D87**, 013004 (2013), arXiv:1212.3805.

[131] C. Kraus, A. Singer, K. Valerius, and C. Weinheimer, Eur.Phys.J. **C73**, 2323 (2013), arXiv:1210.4194.

[132] A. Belesev *et al.*, JETP Lett. **97**, 67 (2013), arXiv:1211.7193.

[133] A. Belesev *et al.*, J.Phys. **G41**, 015001 (2014), arXiv:1307.5687.